Electrically Tunable Slow Light Using Graphene Metamaterials

Kim, Teun-teun; Kim, Hyeon-don; Zhao, Rongkuo; Oh, Sang Soon; Ha, Taewoo; Chung, Dong Seob; Lee, Young Hee; Min, Bumki; Zhang, Shuang

Document Version
Peer reviewed version

Link to publication on Research at Birmingham portal

Electrically tunable slow light using graphene metamaterials

Teun-Teun Kim[1,2], Hyeon-Don Kim[3], Rongkuo Zhao[4], Sang Soon Oh[5], Teawoo Ha[1,2],

Dongsub Chung[1,2], Young Hee Lee[1,2], Bumki Min[3] and Shuang Zhang[6]

[1]*Center for Integrated Nanostructure Physics (CINAP), Institute for Basic Science (IBS), Suwon 16419, Republic of Korea.*

[2]*Sungkyunkwan University, Suwon 16419, Republic of Korea.*

[3]*Department of Mechanical Engineering, Korea Advanced Institute of Science and Technology(KAIST), Daejeon 34141, Republic of Korea*

[4]*NSF Nanoscale Science and Engineering Center, 3112 Etcheverry Hall, University of California, Berkeley, California 94720, USA*

[5]*The Blackett Laboratory, Department of Physics, Imperial College London, South Kensington Campus, London SW7 2AZ, United Kingdom*

[6]*School of Physics and Astronomy, University of Birmingham, Birmingham B15 2TT, United Kingdom*

*Corresponding authors. E-mail: (B. Min) bmin@kaist.ac.kr and (S. Zhang) s.zhang@bham.ac.uk

ABSTRACT

Metamaterials with classical analogues of electromagnetically induced transparency open new avenues in photonics for realizing smaller, more efficient slow light devices without quantum approaches. However, most of the metamaterial based slow light devices are passive, which limits their practical applications. Here, by combining diatomic metamaterials with a gated single-layer graphene, we demonstrate that the group delay of terahertz light can be dynamically controlled under a small gate voltage. Using a two coupled harmonic oscillators model, we show that this active control of group delay is made possible by an effective control of the dissipative loss of the radiative dark resonator by varying the graphene's optical conductivity. Our work may provide opportunities in the design of various applications such as compact slow light devices and ultrasensitive sensors and switches.

Electromagnetically induced transparency (EIT) is a well-known quantum interference phenomenon occurring in coherently driven atomic systems that leads to a sharp cancellation of absorption in the medium[1]. The EIT effect has substantial applications in many fields ranging from nonlinear optics to quantum information technologies[2,3]. Among others, a remarkable feature of EIT is the drastic slow-down of the group velocity of light passing through the medium[4], which enables EIT-based optical memories[5-9]. Slow light has a profound impact on optical science for its ability to enhance light-matter interactions[10-11]. It has great promise in optical communications and optical computation. Remarkably, the

storage time of light up to 1 minute has been demonstrated based on EIT effect in n Pr^{3+}:Y_2SiO_5 crystal[12].

By mimicking the resonant quantum transitions in atomic systems, an EIT-like effect can be observed in classical systems such as electric circuits[13], coupled oscillators[14,15] and plasmonic metamaterials[16-23]. These classical analogues have attracted tremendous attention for their advantage in decreasing the complexity of experimental setups such as laser stability and low-temperature environment. In particular, EIT metamaterial resonators are considered as a promising candidate for realizing bulk slow light devices because of their effective medium characteristics. Furthermore, the ability to dynamically control the EIT-like effect is attractive for practical applications. Recently, it was shown that the EIT-like effect can be dynamically controlled by means of various tuning schemes, such as thermal[24,25], and optical[26-29] methods. As an alternative approach, graphene, an atomically thin layer of carbon atoms arranged in a honeycomb lattice, is an excellent candidate for designing active metamaterials, since its optical conductivity can be controllable through electric gating[30]. Particularly in the terahertz (THz) regime, the electrically controllable density of states available for intra-band transition makes graphene a promising platform for graphene-based active devices such as THz modulators[31-37]. Although significant effort has been devoted to various designs of graphene-based metamaterials for active control of EIT-like effect[38-42], to our knowledge, no experimental result has been reported yet.

In this paper, we demonstrate electrically tunable EIT-like spectral properties by integrating single-layer graphene onto functional unit cells. The EIT resonance is induced by coupling between the bright and dark plasmon modes and can be electrically modulated by changing the damping rate of the dark mode through variation of the optical conductivity of the graphene. As a result, the group delay of THz waves can be effectively controlled by

simply changing the gate voltage, which represents a facile approach for tunable THz optical delay lines, buffer devices and tunable sensors.

RESULTS AND DISCUSSION

As shown schematically in Figure 1a, the graphene EIT metamaterial consists of three functional components: 1) a bi-layer metallic EIT metamaterial, 2) a single-layer graphene, and 3) an ion-gel layer as a gate-dielectric material. A polyimide film is used as a substrate to separate the bi-layer EIT metamaterial. We use a well-studied EIT metamaterial consisting of a pair of split-ring-resonators (SRR) and a cut-wire (CW)[43] with the lattice constants $P_x =$ 104.7 μm and $P_y = 142$ μm. The fabrication of the graphene metasurface device is carried out by standard micro-fabrication techniques. Subsequently a chemical vapor deposition (CVD) grown graphene layer is directly attached to the top layer of the EIT metamaterial by using a wet transfer method[44]. The transferred graphene layer is connected to a gate (**G**) and the ion-gel gate dielectric is connected to a base (**B**) (Figure 1b). During the synthesis and fabrication processes, CVD-grown graphene easily becomes p-doped[45], which is also the case for our graphene samples. A photograph of the fabricated graphene EIT metamaterial is shown in Figure 1c. The metamaterial is characterized by THz time-domain spectroscopy (THz-TDS) giving both amplitude and phase information for transmission coefficients (see Methods for details).

In order to clarify the mechanism of the graphene EIT metamaterial, we first perform numerical simulations using the commercially available finite element method (FEM) solver (see Methods for details). The simulated transmission amplitude of only CW array (bright blue curve) and SRR-pair array (pink curve) are shown in Figure 1d. The typical plasmonic dipole (PD) resonance in the CW can be excited directly by the incident THz wave, while an

inductive-capacitive (LC) resonance in the SRR-pair cannot be exited directly due to the perpendicular orientation of the electric field of the incident THz wave. Thus, the CW and SRR-pair serve as the bright and dark resonators, respectively. In the EIT metamaterial, the near-field coupling between the bright and dark resonators excite the LC resonance in the dark atom as shown in Figure 1e. As a result, the destructive interference between the PD and LC resonances leads to a sharp transparency peak at 0.85 THz.

Figure 2a shows the measured and simulated transmission amplitude spectra of the graphene EIT metamaterial as a function of the gate voltages applied to graphene layer. After transferring the graphene and ion-gel onto the SRR-pair array, it is shown that the EIT peak is red-shifted and the transmission amplitude T decreases due to the intrinsic conductivity of the graphene layer and dielectric loss of ion-gel that damp the LC resonance of the dark resonator. However, the EIT feature persists with more than 51 % of transmission amplitude at 0.75 THz. A higher transparency peak may be achievable if the graphene layer is patterned and covered only on the gap of SPP-pair or ion-gel dielectric thickness is reduced. The gate voltage relative to charge neutral point $\Delta V = V_\mathrm{g} - V_\mathrm{CNP}$ determines the doping level of graphene. The damping rate of the dark resonance is actively controlled by the gate voltage that determines the conductivity of graphene layer. It is shown that the transparency peak can be gradually reduced by increasing the applied voltage. The maximum amplitude modulation depth, defined as a relative transmission change $\Delta T / T_\mathrm{CNP}$ for graphene EIT metamaterial, is measured to be 25 % at the frequency 0.75 THz.

To interpret the mechanism of electrical tuning mechanism observed in the experiments, the optical conductivity of single-layer graphene σ in the THz regime is calculated via Kubo formula as a function of the Fermi energy E_F[46]. The applied gate voltage is related to the Fermi energy of graphene as $|E_F| = \hbar v_F(\pi N)^{1/2}$. Here, $\hbar = h/2\pi$ is the Plank constant, v_F

is the Fermi velocity, N is the total carrier density given by $N = (n_0^2 + \alpha^2 |\Delta V|^2)^{1/2}$, and $\alpha \approx 8.0 \times 10^{11}$ cm^{-2}V^{-1} is the gate capacitance of the ion gel, respectively. It is assumed that the intra-band scattering time $\tau = 16$ fs and the carrier density at the conductivity minimum is $n_0 = 5.4 \times 10^{10}$ cm^2. By applying these values into the Kubo formula, transmission amplitude T is calculated as a function of gate voltage. As clearly seen from the plot in Figure 2, the simulation results show an excellent agreement with the measured data. In order to understand the gate-dependent modulation characteristics, measured transmission amplitude at the EIT resonance frequency 0.75 THz are plotted in Figure 2c as a function of $|\Delta V|^{1/2}$ and compared with the simulation results. The result clearly shows that the transmission amplitude is proportional to the square root of the gate voltage[32].

Figure 3 shows the calculated electric field for the unit cell of the graphene EIT metamaterial at two different gate voltages of $\Delta V = 0.0$ V and $\Delta V = 1.7$ V at 0.75 THz. Without applying the gate-voltage, the graphene layer is mainly dielectric and the electric field is primarily concentrated around the SRR-pair gap due to the indirect excitation through the coupling with the CW, whereas the electric field in the CW is completely suppressed, which is the characteristic of a typical EIT effect (Figure 3a). With the increase of the conductivity of graphene, the LC resonance in the SRR-pair is strongly damped and therefore the electric field in the SRR-pair gaps is suppressed. As a result the field is localized at the end of CW only, as shown in the case of $\Delta V = 1.7$ V (Figure 3b).

The gate-controlled transmission properties of graphene EIT metamaterial is utilized to validate the active modulation of the slow light behavior. The slow light performance is characterized by the group delay for the pulses, $t_g = -d\phi/d\omega$, where ϕ is the phase and ω is the angular frequency of the THz pulse. The measured and simulated relative changes in t_g is plotted in Fig. 4 as a function of the gate voltage from $\Delta V = -0.3$ V to $\Delta V = 1.7$ V. The

wave pulse with central frequency 0.75 THz is delayed by 3.1 ps in the case of $\Delta V = 0.0$ V, which is equivalent to the time delay of a 0.63 mm distance of free space propagation. Moreover, a remarkably wide tuning range of 3.3 ps is obtained within only 1.7 V of gate voltage. This low energy operation of controlled reduction in the speed of light is highly desirable in practical applications, such as regenerators for THz communication and compact tunable THz delay lines.

Next, a coupled harmonic oscillator model[47] is used to explain the physical origin of active modulation of coupling effect between bright and dark modes in the graphene EIT metamaterial:

$$\omega_B^{-2}\ddot{p}(t) + \Gamma_B\omega_B^{-1}\dot{p}(t) + p(t) = f(t) - \kappa q(t),$$

$$\omega_D^{-2}\ddot{q}(t) + \Gamma_D\omega_D^{-1}\dot{q}(t) + q(t) = -\kappa p(t), \tag{1}$$

where ω_B, ω_D, Γ_B, and Γ_D are resonance frequencies and damping factors of the bright and dark resonators respectively. Γ_B and Γ_D are described by the excitation $p(t)$ and $q(t)$ respectively, and Γ_B is driven by the external driving force $f(t)$. The two resonators are linearly coupled with a coupling strength κ. Equation (1) can be solved in the frequency domain by assuming a solution of the form $p(t) = \tilde{p}(\omega)\exp(-i\omega t)$ and $q(t) = \tilde{q}(\omega)\exp(-i\omega t)$:

$$\tilde{p}(\omega) = \frac{\Delta_D(\omega)\tilde{f}(\omega)}{\Delta_D(\omega)\Delta_B(\omega)-\kappa^2},$$

$$\tilde{q}(\omega) = \frac{\kappa\tilde{f}(\omega)}{\Delta_D(\omega)\Delta_B(\omega)-\kappa^2}, \tag{2}$$

where $\Delta_{D,B}(\omega) = 1 - (\omega/\omega_{D,B})^2 - i\Gamma_D(\omega/\omega_{D,B})$. The single unit of the EIT metamaterial can be approximately described by an electric current sheet with surface conductivity:

$$\sigma_{\text{se}} \approx \varepsilon_0 \chi_{se}^{(\text{static})} \frac{-i\omega\tilde{p}(\omega)}{\tilde{f}(\omega)} = \frac{-i\omega\beta\Delta_D(\omega)}{\Delta_D(\omega)\Delta_B(\omega)-\kappa^2}, \tag{3}$$

where χ_{se} is the surface susceptibility and $\beta \equiv \epsilon_0 \chi_{se}^{(static)}$. Then the transmission coefficient of the EIT metamaterial T is given by:

$$T = \frac{2}{2 + \eta_0 \sigma_{se}} \tag{4}$$

where η_0 is the wave impedance in free space. The green lines in Fig. 2b represent the analytically fitted transmission spectra using equation (4) as a function of the gate voltage. As clearly seen from the plot in Fig. 2b, the theoretical results show very good agreement with both the experimental and simulation results. The corresponding fitting parameters for $\omega_{B,D}$, $\Gamma_{B,D}$, and κ are plotted in Fig. 5 as a function of gate voltage ΔV. As expected, the damping factor Γ_D increases significantly as ΔV increases, which indicates that the increasing ΔV affects the resonance strength of the dark mode. The coupling coefficient κ also increases as ΔV increases, implying weaker excitation $q(t)$ in dark resonator.

CONCLUSION

In conclusion, we have experimentally demonstrated an electrically tunable graphene EIT metamaterial which showed substantial modulation of transmission peak at the THz regime. Theoretical analysis based on the two coupled harmonic oscillators model verifies that this active EIT switching is attributed to the suppression of resonance strength for the dark mode by varying the optical conductivity of graphene. In addition, from the measurement, we validated that the graphene EIT metamaterial achieved a very large group delay modulation up to 3.3 ps within low gate voltage. Benefitting from the electric control of EIT effect, the proposed graphene EIT metamaterials may provide opportunities in the design of various applications such as compact slow light devices, ultrasensitive sensors and nonlinear devices with low energy operation.

MATERIALS AND METHODS

Fabrication procedure for a graphene EIT metamaterial.

Firstly, the metallic metamaterial array was fabricated using conventional micro-fabrication techniques. Polyimide solution (PI-2610, HD MicroSystems) was spin-coated on a silicon wafer, and cured subsequently two-step baking process in a convection oven and a furnace. As a first CW layer, a 300-nm-thick gold was deposited with a 10-nm-thick chromium adhesion layer on the negative photoresist (AZ nLOF 2035, MicroChemicals), which was patterned by photolithography. After the lift-off process, the CW layer was defined. To separate the SRR-pair layer from the CW layer, the same polyimide curing process was repeated but with a different thickness of 5 µm. On top of a spacer, SRR-pair and a square ring-shaped graphene electrode were defined following the same process which was used for the first layer. At the same time, a side-gate electrode was employed beside the graphene electrode to simplify the fabrication process. Next, commercial CVD-grown monolayer graphene on a copper film (Graphene Square) was transferred to the entire area covering the second double Z metamaterial (5×5 mm^2) and the surrounding graphene electrode. We used a conventional wet-based transfer method using a thermal release tape as a supporting layer. Finally, as a gate dielectric, we employed a 20-µm-thick ion gel using the cut and stick method. The ion gel solution was prepared by dissolving P(VDF-HFP) and [EMI][TFSA] in acetone with the weight ratio of 1:4:7. This solution was dried in a vacuum oven at a temperature of 70°C during 24 hours. The cured ion gel was cut with a razor blade and then transferred between two electrodes. Finally, the thin flexible graphene CDZM was peeled off from the silicon substrate, and attached to a holed PCB substrate.

THz-TDS measurements

To generate broadband THz waves, we used a GaAs photoconductive antenna (iPCA, BATOP) as terahertz emitter illuminated by a femtosecond Ti:sapphire laser (Mai-Tai, Spectra-physics) with a central wavelength of 800 nm and 80 MHz repetition rate, respectively. An electro-optic sampling method with ZnTe crystal of 1 mm thickness was used to detect the transmitted THz signals in the time domain. The THz-TDS system has a usable bandwidth of 0.1 - 2.0 THz.

Numerical modelling

The numerical simulation were carried out using commercially available FEM solver of CST Microwave Studio. Frequency-dependent material parameters of gold, polyimide, and ion gel at THz frequencies were experimentally determined. The sheet conductivity of graphene in the THz regime can be derived using the well-known Kubo formula, which described with only intraband contributions,

$$\sigma_{intra}(\omega) = \frac{e^2}{\pi\hbar^2}\frac{i}{\omega+i\tau^{-1}}\int_{\Delta}^{\infty}d\epsilon\left(1+\frac{\Delta^2}{\epsilon^2}\right)[f(\epsilon-E_{\mathrm{F}})+f(\epsilon+E_{\mathrm{F}})],$$

where, e and $\hbar$ are universal constants representing the electron charge and Plank's constant, and E_F, τ, and Δ are Fermi energy, the momentum relaxation time, and half bandgap energy from the tight-binding Hamiltonian near K points of the Brillouin zone, respectively.

ASSOCIATED CONTENT

The Supporting Information is available free of charge on the Internet at http://pubs.acs.org.

AUTHORS' INFORMATION

Corresponding authors:

[*]bmin@kaist.ac.kr

[*]s.zhang@bham.ac.uk

REFERENCES

(1)   Harris, S. E. *Electromagnetically induced transparency*. *Phys. Today* **1997**, 50, 36-42.

(2)   Fleischhauer, M.; Imamoglu, A.; Marangos, J. Electromagnetically induced transparency: Optics in coherent media. *J. Rev. Mod. Phys.* **2005** 77, 633.

(3)   Marangos, J. P.; Halfmann, T. *Handbook of Optics*. McGraw-Hill, New York, **2009**.

(4)   Hau, L. V.; Harris, S. E.; Dutton, Z.; Behroozi, C. H. Stopped light and image storage by electromagnetically induced transparency up to the regime of one minute *Nature* **1999**, 397, 594-598.

(5)   Liu, C.; Dutton, Z.; Behroozi, C. H.; Hau, L. V. Observation of coherent optical information storage in an atomic medium using halted light pulses *Nature* **2001** 409 490-493.

(6)   Turukhin, A. V. *et al.* Observation of ultraslow and stored light pulses in a solid. *Phys. Rev. Lett.* **2001**, 88, 023602.

(7)   Chaneliere, T. *et al.* Storage and retrieval of single photons transmitted between remote quantum memories. *Nature* **2005**, 438, 833–836.

(8)   Vudyasetu, P. K., Camacho, R. M. & Howell, J. C. Storage and retrieval of multimode transverse images in hot atomic rubidium vapor. *Phys. Rev. Lett.* **2008**, 100, 123903.

(9)   Shuker, M.; Firstenberg, O.; Pugatch, R.; Ron, A.; Davidson, N. Storing Images in Warm Atomic Vapor. *Phys. Rev. Lett.* **2008**, *100* (22), 223601.

(10)   Krauss, T. F. Why Do We Need Slow Light? *Nature* **2008**, *2* (8), 448–450.

(11)   Beggs, D. M.; White, T. P.; O'Faolain, L.; Krauss, T. F. Ultracompact and Low-Power Optical Switch Based on Silicon Photonic Crystals. *Opt. Lett.* **2008**, *33* (2), 147–149.

(12) Heinze, G.; Hubrich, C.; Halfmann, T. Stopped Light and Image Storage by Electromagnetically Induced Transparency Up to the Regime of One Minute. *Phys. Rev. Lett.* **2013**, *111* (3), 033601.

(13) Garrido Alzar, C. L.; Martinez, M. A. G.; Nussenzveig, P. Classical Analog of Electromagnetically Induced Transparency. *Am. J. Phys.* **2002**, *70* (1), 37.

(14) Xu, Q.; Sandhu, S.; Povinelli, M.; Shakya, J.; Fan, S.; Lipson, M. Experimental Realization of an on-Chip All-Optical Analogue to Electromagnetically Induced Transparency. *Phys. Rev. Lett.* **2006**, *96* (12), 123901.

(15) Yang, X.; Yu, M.; Kwong, D.-L.; Wong, C. All-Optical Analog to Electromagnetically Induced Transparency in Multiple Coupled Photonic Crystal Cavities. *Phys. Rev. Lett.* **2009**, *102* (17), 173902.

(16) Zhang, S.; Genov, D. A.; Wang, Y.; Liu, M.; Zhang, X. Plasmon-Induced Transparency in Metamaterials. *Phys. Rev. Lett.* **2008**, *101* (4), 047401.

(17) Papasimakis, N.; Fedotov, V.; Zheludev, N.; Prosvirnin, S. Metamaterial Analog of Electromagnetically Induced Transparency. *Phys. Rev. Lett.* **2008**, *101* (25), 253903.

(18) Tassin, P.; Zhang, L.; Koschny, T.; Economou, E.; Soukoulis, C. Low-Loss Metamaterials Based on Classical Electromagnetically Induced Transparency. *Phys. Rev. Lett.* **2009**, *102* (5), 053901.

(19) Liu, N.; Langguth, L.; Weiss, T.; Kästel, J.; Fleischhauer, M.; Pfau, T.; Giessen, H. Plasmonic Analogue of Electromagnetically Induced Transparency at the Drude Damping Limit. *Nat Mater* **2009**, *8* (9), 758–762.

(20) Kekatpure, R. D.; Barnard, E. S.; Cai, W.; Brongersma, M. L. Phase-Coupled Plasmon-Induced Transparency. *Phys. Rev. Lett.* **2010**, *104* (24), 243902.

(21) Zhang, L.; Tassin, P.; Koschny, T.; Kurter, C.; Anlage, S. M.; Soukoulis, C. M. Large Group Delay in a Microwave Metamaterial Analog of Electromagnetically Induced Transparency. *Appl. Phys. Lett.* **2010**, *97* (24), 241904.

(22) Jung, H.; In, C.; Choi, H.; Lee, H. Electromagnetically Induced Transparency Analogue by Self-Complementary Terahertz Meta-Atom. *Advanced Optical Materials* **2016**, *4* (4), 627–633.

(23) Liu, X.; Gu, J.; Singh, R.; Ma, Y.; Zhu, J.; Tian, Z.; He, M.; Han, J.; Zhang, W. Electromagnetically Induced Transparency in Terahertz Plasmonic Metamaterials via Dual Excitation Pathways of the Dark Mode. *Appl. Phys. Lett.* **2012**, *100* (13), 131101.

(24) Kurter, C.; Tassin, P.; Zhang, L.; Koschny, T.; Zhuravel, A. P.; Ustinov, A. V.; Anlage, S. M.; Soukoulis, C. M. Classical Analogue of Electromagnetically Induced Transparency with a Metal-Superconductor Hybrid Metamaterial. *Phys. Rev. Lett.* **2011**, *107* (4), 043901.

(25) Cao, W.; Singh, R.; Zhang, C.; Han, J.; Tonouchi, M.; Zhang, W. Plasmon-Induced Transparency in Metamaterials: Active Near Field Coupling Between Bright Superconducting and Dark Metallic Mode Resonators. *Appl. Phys. Lett.* **2013**, *103* (10), 101106–101106.

(26) Gu, J.; Singh, R.; Liu, X.; Zhang, X.; Ma, Y.; Zhang, S.; Maier, S. A.; Tian, Z.; Azad, A. K.; Chen, H.-T.; Taylor, A. J.; Han, J.; Zhang, W. Active Control of Electromagnetically Induced Transparency Analogue in Terahertz Metamaterials. *Nature Communications* **2012**, *3*, 1151–1156.

(27) Roy Chowdhury, D.; Singh, R.; Taylor, A. J.; Chen, H.-T.; Azad, A. K. Ultrafast Manipulation of Near Field Coupling Between Bright and Dark Modes in Terahertz Metamaterial. *Appl. Phys. Lett.* **2013**, *102* (1), 011122–011126.

(28) Miyamaru, F.; Morita, H.; Nishiyama, Y.; Nishida, T.; Nakanishi, T.; Kitano, M.; Takeda, M. W. Ultrafast Optical Control of Group Delay of Narrow-Band Terahertz Waves. *Sci. Rep.* **2014**, *4*, 97–5.

(29) Su, X.; Ouyang, C.; Xu, N.; Tan, S.; Gu, J.; Tian, Z.; Singh, R.; Zhang, S.; Yan, F.; Han, J.; Zhang, W. Dynamic Mode Coupling in Terahertz Metamaterials. *Sci. Rep.* **2015**, 1–10.

(30) Castro Neto, A. H.; Guinea, F.; Peres, N. M. R.; Novoselov, K. S.; Geim, A. K. The Electronic Properties of Graphene. *Rev. Mod. Phys.* **2009**, *81* (1), 109–162.

(31) Gusynin, V. P.; Sharapov, S. G.; Carbotte, J. P. Ac Conductivity of Graphene: From Tight-Binding Model to 2+1-Dimension Electrodynamics. *International Journal of Modern Physics B* **2007**, *21* (27), 4611–4658.

(32) Lee, S. H.; Choi, M.; Kim, T.-T.; Lee, S.; Liu, M.; Yin, X.; Choi, H. K.; Lee, S. S.; Choi, C.-G.; Choi, S. Y.; Zhang, X.; Min, B. Switching Terahertz Waves with Gate-Controlled Active Graphene Metamaterials. *Nat Mater* **2012**, *11* (11), 936–941.

(33) Valmorra, F.; Scalari, G.; Maissen, C.; Fu, W.; Schönenberger, C.; Choi, J. W.; Park, H. G.; Beck, M.; Faist, J. Low-Bias Active Control of Terahertz Waves by Coupling

Large-Area CVD Graphene to a Terahertz Metamaterial. *Nano Lett.* **2013**, *13* (7), 3193–3198.

(34) Gao, W.; Shu, J.; Reichel, K.; Nickel, D. V.; He, X.; Shi, G.; Vajtai, R.; Ajayan, P. M.; Kono, J.; Mittleman, D. M.; Xu, Q. High-Contrast Terahertz Wave Modulation by Gated Graphene Enhanced by Extraordinary Transmission Through Ring Apertures. *Nano Lett.* **2014**, *14* (3), 1242–1248.

(35) Miao, Z.; Wu, Q.; Li, X.; He, Q.; Ding, K.; An, Z.; Zhang, Y.; Zhou, L. Widely Tunable Terahertz Phase Modulation with Gate-Controlled Graphene Metasurfaces. *Phys. Rev. X* **2015**, *5* (4), 041027–13.

(36) Liu, P. Q.; Luxmoore, I. J.; Mikhailov, S. A.; Savostianova, N. A.; Valmorra, F.; Faist, J.; Nash, G. R. Highly Tunable Hybrid Metamaterials Employing Split-Ring Resonators Strongly Coupled to Graphene Surface Plasmons. *Nature Communications*. **2015**, 6, 8969.

(37) Kim, T.-T.; Oh, S. S.; Kim, H.-D.; Park, H.-S.; Hess, O.; Min, B.; Zhang, S. Electrical Access to Critical Coupling of Circularly Polarized Waves in Graphene Chiral Metamaterials. *Science Advances* **2017**, *3* (9), e1701377.

(38) Jiang, J.; Zhang, Q.; Ma, Q.; Yan, S.; Wu, F.; He, X. Dynamically Tunable Electromagnetically Induced Reflection in Terahertz Complementary Graphene Metamaterials. *Opt. Mater. Express* **2015**, *5* (9), 1962–10.

(39) Zhao, X.; Yuan, C.; Lv, W.; Xu, S.; Yao, J. Plasmon-Induced Transparency in Metamaterial Based on Graphene and Split-Ring Resonators. *IEEE Photon. Technol. Lett.* **2015**, *27* (12), 1321–1324.

(40) Fu, G.-L.; Zhai, X.; Li, H.-J.; Xia, S.-X.; Wang, L.-L. Dynamically Tunable Plasmon Induced Transparency in Graphene Metamaterials. *J. Opt.* **2016**, *19* (1), 015001–015007.

(41) Zhang, H.; Zhang, X.; Cao, Y.; Zeng, B.; Zhou, M.; Zhang, Y. Tunable Terahertz Electromagnetically Induced Transparency Based on a Complementary Graphene Metamaterial. *Mater. Res. Express* **2017**, *4* (1), 015002–015010.

(42) Zhao, X.; Yuan, C.; Zhu, L.; Yao, J. Graphene-Based Tunable Terahertz Plasmon-Induced Transparency Metamaterial. *Nanoscale* **2016**, *8* (33), 15273–15280.

(43) Liu, X.; Gu, J.; Singh, R.; Ma, Y.; Zhu, J.; Tian, Z.; He, M.; Han, J.; Zhang, W. Electromagnetically Induced Transparency in Terahertz Plasmonic Metamaterials via Dual Excitation Pathways of the Dark Mode. *Appl. Phys. Lett.* **2012**, *100* (13), 131101.

(44) Li, Q.; Tian, Z.; Zhang, X.; Singh, R.; Du, L.; Gu, J.; Han, J.; Zhang, W. Active Graphene-Silicon Hybrid Diode for Terahertz Waves. *Nature Communications* **2015**, *6*.

(45) Pirkle, A.; Chan, J.; Venugopal, A.; Hinojos, D.; Magnuson, C. W.; McDonnell, S.; Colombo, L.; Vogel, E. M.; Ruoff, R. S.; Wallace, R. M. The Effect of Chemical Residues on the Physical and Electrical Properties of Chemical Vapor Deposited Graphene Transferred to SiO 2. *Appl. Phys. Lett.* **2011**, *99* (12), 122108–4.

(46) Gusynin, V. P.; Sharapov, S. G.; Carbotte, J. P. Ac Conductivity of Graphene: From Tight-Binding Model to 2+1-Dimension Electrodynamics. *International Journal of Modern Physics B* **2007**, *21* (27), 4611–4658.

(47) Tassin, P.; Zhang, L.; Zhao, R.; Jain, A.; Koschny, T.; Soukoulis, C. M. Electromagnetically Induced Transparency and Absorption in Metamaterials: the Radiating Two-Oscillator Model and Its Experimental Confirmation. *Phys. Rev. Lett.* **2012**, *109* (18), 187401–187405.
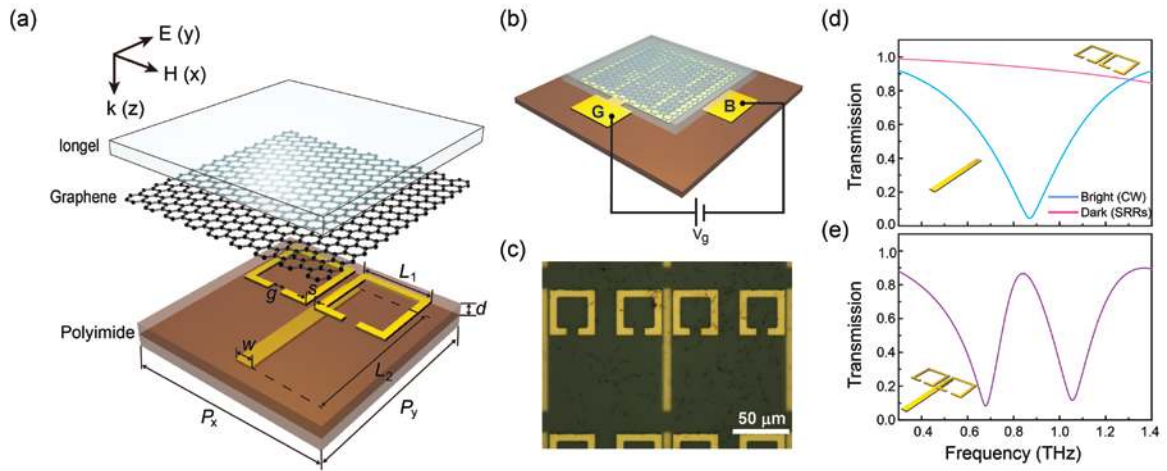
Figure 1. (a) Schematic view of gate-controlled active graphene EIT composed of a split-ring resonator (SRR) pair and a cut wire (CW). A single layer graphene deposited on the layer of SRRs and subsequently covered by a layer of ion gel gate dielectric (t_{ion} = 20 µm). The geometry parameters are given as L_1 = 40.0 μm, L_2 = 122.0 μm , w = 8.0 μm, g = 5.0 μm, s = 4.7 μm, l = 20 μm, d = 5 μm, P_x = 104.7 μm and P_y = 142 μm, and a thickness of embedded dielectric material (Polyimide) d = 5.0 μm. (b) Schematic rendering of the fabricated graphene EIT metamaterial. The graphene layer is connected to a gate **G** and the ion gel gate dielectric is connected to a base **B**. (c) Top-view microscopic image of the fabricated graphene EIT metamaterial. (d) Simulated transmission amplitude for (top) CW and SRR-pair as a bright and dark atom respectively, and (bottom) EIT metamaterial without graphene and ion gel layer.
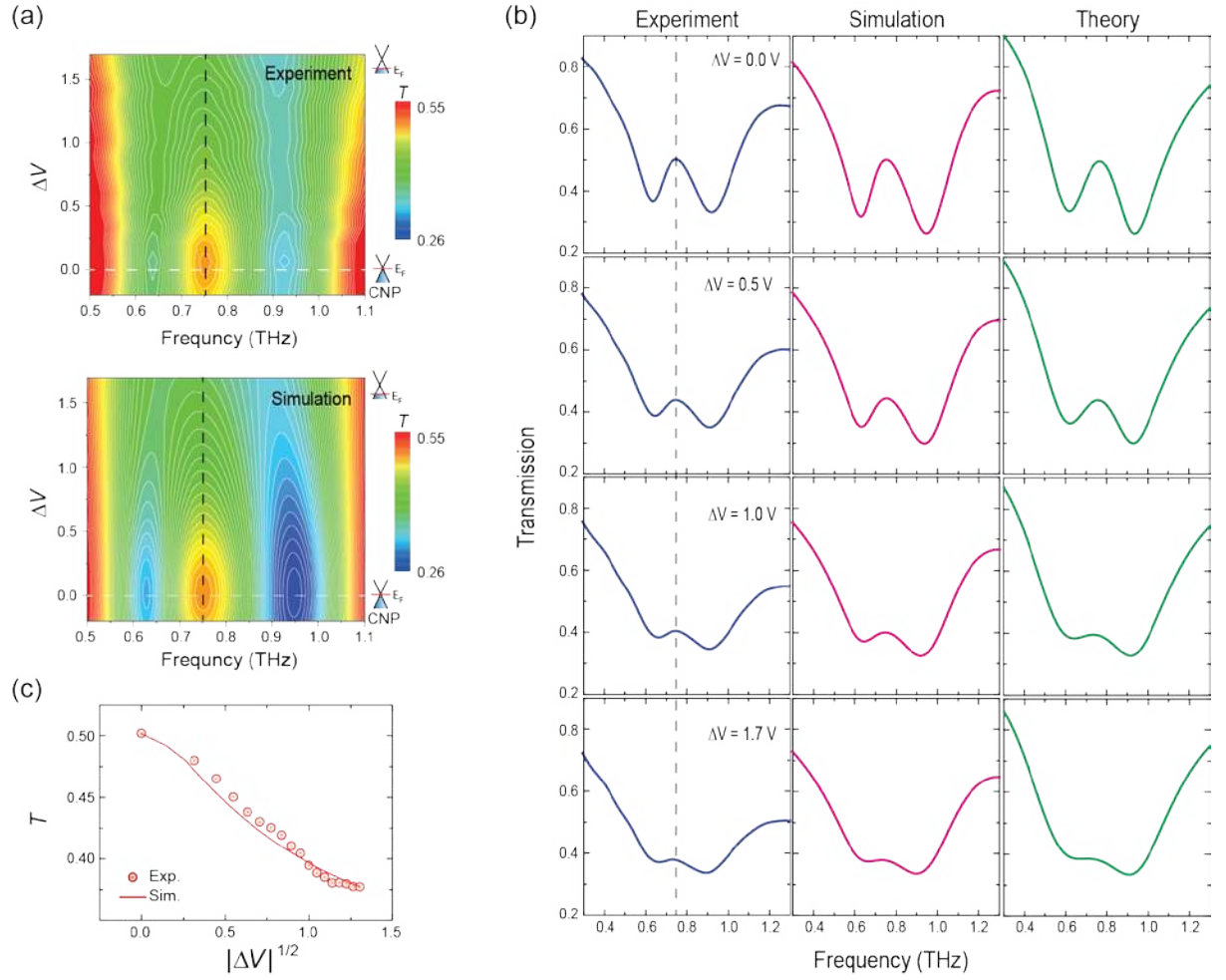
Figure 2. (a) Measured and simulated amplitude of transmission spectra obtained by experimental measurements and numerical simulation as a function of ΔV. (b) Comparison of transmission amplitude between measured, simulated and theoretical fitting obtained from the two coupled harmonic oscillators with four different gate voltages. (c) Measured transmission amplitude (scatter) plotted as a function of $|\Delta V|^{1/2}$ along with the simulated result (line) at the frequency 0.75 THz.
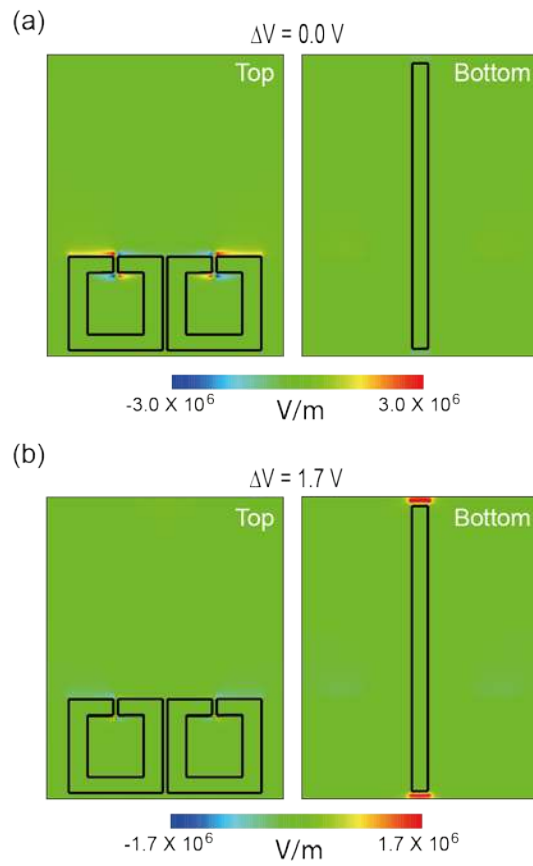
Figure 3. Electric field concentration in the EIT metamaterials with gate voltage ΔV equal to (a) 0 V and (b) 1.7 V at the frequency 0.75 THz.
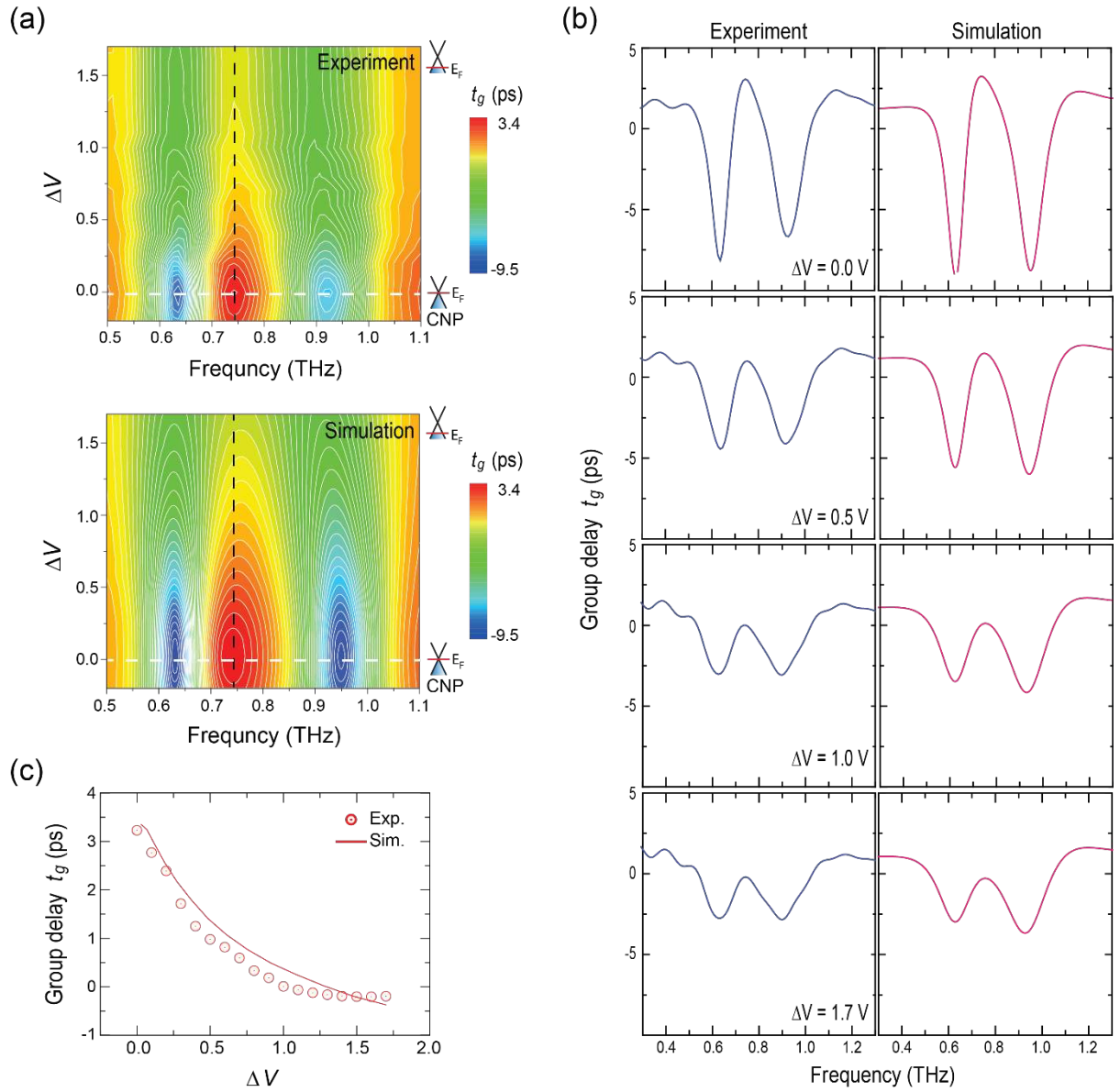
Figure 4. (a) Measured and simulated group delay t_g as a function of ΔV. (b) Comparison between measured and simulated group delay t_g with four different gate voltages. (c) Measured transmission amplitude (scatter) plotted as a function of ΔV along with the simulated result (line) at the frequency 0.75 THz.
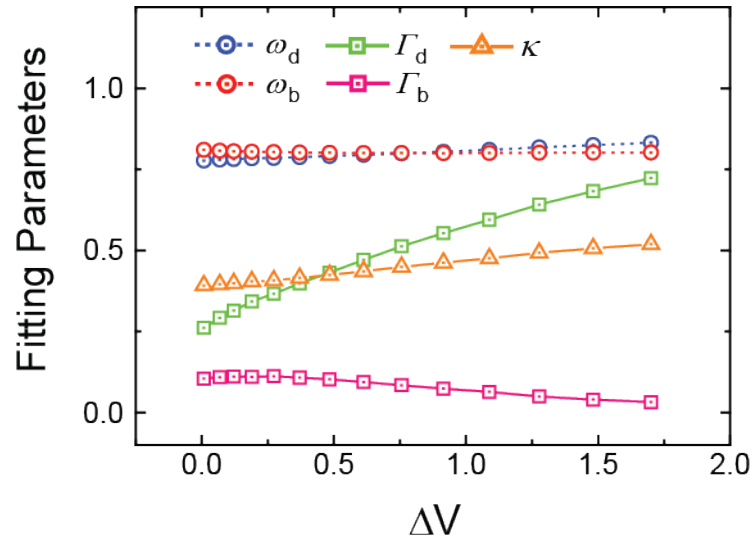
Figure 5. The values of fitting parameters ω_B, ω_D, Γ_B, Γ_D, and κ used in the two coupled harmonic oscillators model as a function of ΔV.

SYNOPSIS